Supplemental Document

Biomedical Optics EXPRESS

Axial resolution improvement of two-photon microscopy by multi-frame reconstruction and adaptive optics: supplement

SHIWEI YE,[1,2] YIXUAN YIN,[1,2] JING YAO,[1,2] JUN NIE,[3] YUCHEN SONG,[1,4] YUFENG GAO,[1,2] JIA YU,[1,2] HUI LI,[1,2] PENG FEI,[3,5] AND WEI ZHENG[1,2,6]

[1]*Research Laboratory for Biomedical Optics and Molecular Imaging, Shenzhen Institutes of Advanced Technology, Chinese Academy of Sciences, Shenzhen 518055, China*
[2]*CAS Key Laboratory of Health Informatics, Shenzhen Institutes of Advanced Technology, Chinese Academy of Sciences, Shenzhen 518055, China*
[3]*School of Optical and Electronic Information, Huazhong University of Science and Technology, Wuhan 430074, China*
[4]*Department of Biomedical Engineering, The Hong Kong Polytechnic University, Hong Kong SAR, China*
[5]*feipeng@hust.edu.cn*
[6]*zhengwei@siat.ac.cn*

Supplement DOI: https://doi.org/10.6084/m9.figshare.13110956

Parent Article DOI: https://doi.org/10.1364/BOE.409651

Supplementary Information

Axial resolution improvement of two-photon microscopy by multi-frame reconstruction and adaptive optics

SHIWEI YE,[1,2] YIXUAN YIN,[1,2] JING YAO,[1,2] JUN NIE,[3] YUCHEN SONG,[1,4] YUFENG GAO,[1,2] JIA YU,[1,2] HUI LI,[1,2] PENG FEI,[3,5,*] AND WEI ZHENG[1,2,6,*]

[1]Research Laboratory for Biomedical Optics and Molecular Imaging, Shenzhen Institutes of Advanced Technology, Chinese Academy of Sciences, Shenzhen 518055, China

[2]CAS Key Laboratory of Health Informatics, Shenzhen Institutes of Advanced Technology, Chinese Academy of Sciences, Shenzhen 518055, China

[3]School of Optical and Electronic Information, Huazhong University of Science and Technology, Wuhan 430074, China

[4]Department of Biomedical Engineering, The Hong Kong Polytechnic University, Hong Kong SAR, China

[5]feipeng@hust.edu.cn

[6]zhengwei@siat.ac.cn

**corresponding author*

This document provides supplementary information to "Axial resolution improvement of two-photon microscopy by multi-frame reconstruction and adaptive optics". This includes additional notes and data.

Supplementary Note 1: Typical number (*n*) of low-resolution volumes for multi-frame reconstruction (MR)

As show in Fig. S1, different n were tested and compared for the same raw data by measuring 200-nm fluorescent beads. The axial resolution of the developed TPM system was ~3.5 μm, and thus d was set as 1.52 μm to satisfy the Nyquist sampling principle. The oversampling steps are 0.76 μm for n = 2, 0.38 μm for n = 4, and 0.19 μm for n = 8, respectively. The measured volume was 27.3 × 27.3 × 40 μm^3. It is found that the axial FWHMs was improved when n was changed from 2 to 4, while the axial profile of n = 4 is basically in agreement with that of n = 8. The results suggested n = 4 is most likely to provide the optimal balance between the reconstruction accuracy and efficiency.

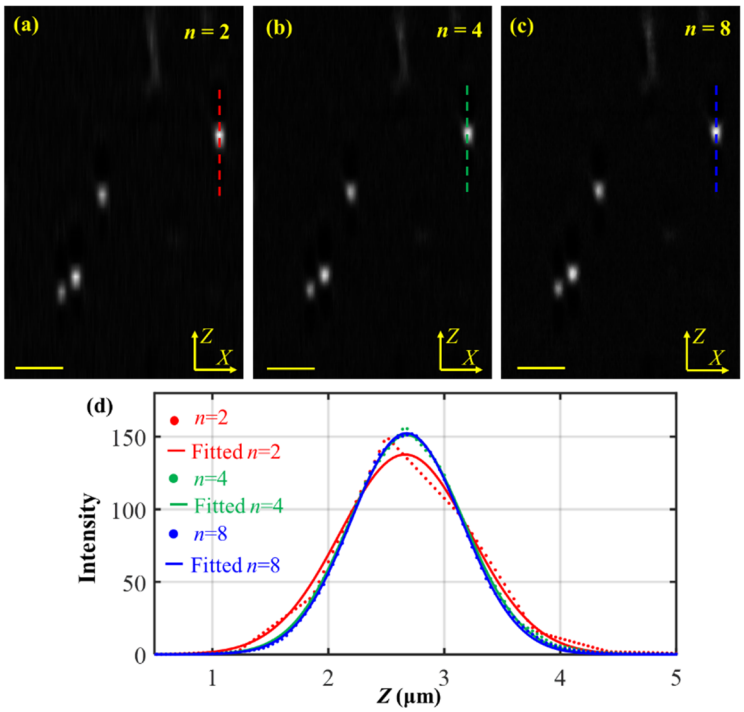

Fig. S1. Reconstructed *XZ* planes of 200-nm fluorescent beads under different number (*n*) of low-resolution volumes. (a) *n* =2. (b) *n* = 4. (c) *n*=8. (d) Intensity comparison of one cross section using different *n*. Scale bars: 5 μm (a–c)

Supplementary Note 2: The validity of the sensorless AO during the liquid lens focusing

As shown in Fig. S2, we measured 200-nm fluorescent beads and compared the lateral views between AO off and AO on at five different axial positions. Furthermore, the corresponding lateral cross-sections (indicated as red dashed lines for AO off and green dashed lines for AO on) were plotted. The results suggested that the sensorless AO can effectively improve the peak intensity of measured fluorescent beads and enhance the lateral resolution during the liquid lens focusing.

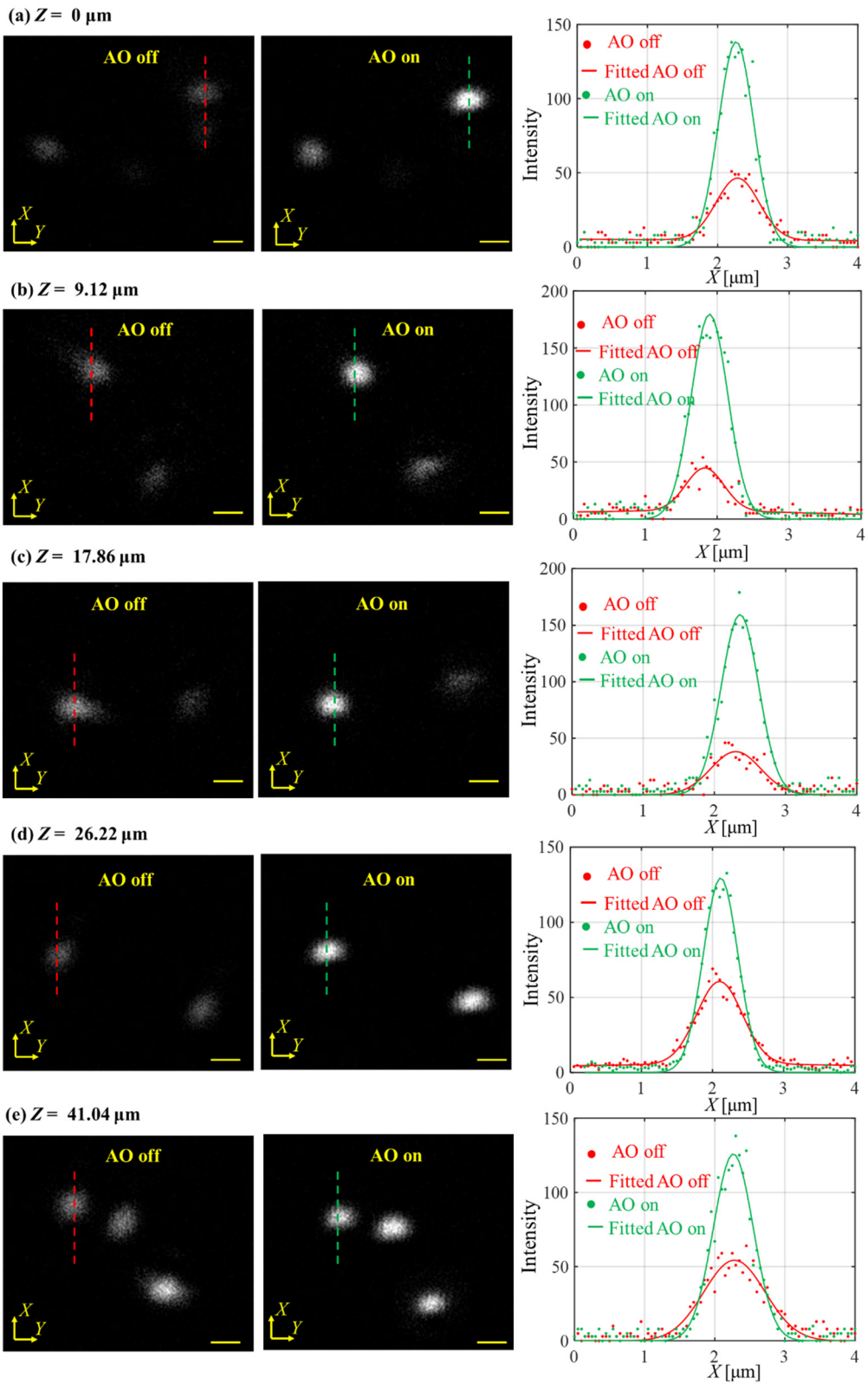
(a) Z = 0 µm
AO off
AO on
(b) Z = 9.12 µm
AO off
AO on
(c) Z = 17.86 µm
AO off
AO on
(d) Z = 26.22 µm
AO off
AO on
(e) Z = 41.04 µm
AO off
AO on
X
Y
AO off
Fitted AO off
AO on
Fitted AO on
Intensity
X [µm]

Fig. S2. Lateral views and intensity comparisons between AO off and AO on at different depths adjusted by the liquid lens. (a) $Z = 0$ μm. (b) $Z = 9.12$ μm. (c) $Z = 17.86$ μm. (d) $Z = 26.22$ μm. (e) $Z = 41.04$ μm. Scale bars: 1 μm (a–c)

Supplementary Note 3: Comparison between the proposed MR algorithm and only deconvolution process

A comparison between the proposed MR algorithm and only deconvolution process was provided, as show in Fig. S3. 200-nm fluorescent beads were imaged in a volume of $27.3 \times 27.3 \times 45.6$ μm^3 with the $512 \times 512 \times 120$ pixels, and the entire volume was divided into four axially related low-resolution volumes ($n = 4$, $l = 0.38$ μm). The deconvolution process was based on maximum likelihood estimation, which was the same as O_k^T in the proposed MR algorithm. It is no doubt that the deconvolution process can improve the axial resolution (comparison between red and green lines in Fig. S3). However, with the proposed MR algorithm, the axial resolution can be further improved (blue line in Fig. S3). Because the proposed MR algorithm not only deals with the problem of the optical blur of imaging system, but incorporates the inverse operations of motion effect and down-sampling effect.

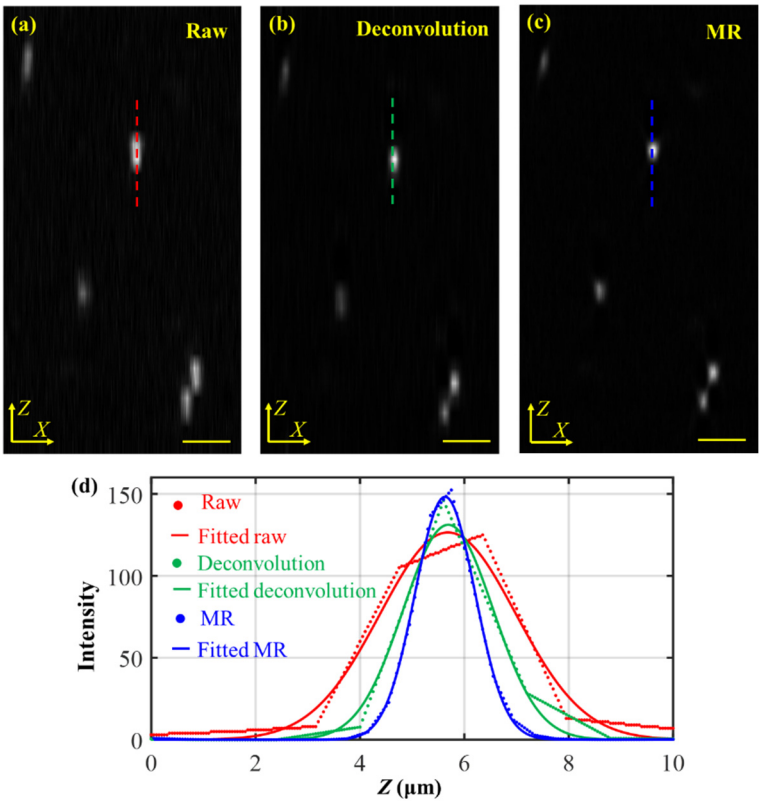

Fig. S3. *XZ* planes of 200-nm fluorescent beads with different process methods. (a) Raw data. (b) By only deconvolution process. (c) By the proposed MR algorithm. (d) Intensity comparison of one cross section using the three methods. Scale bars: 5 μm (a–c)